POLITECNICO
MILANO 1863

SCUOLA DI INGEGNERIA INDUSTRIALE
E DELL'INFORMAZIONE

Executive Summary of the Thesis

Towards the detection of ultra-low energetic neutrinos with plasma metamaterials

Laurea Magistrale in Engineering Physics

Author: Carlo Alfisi

Advisor: Prof. Matteo Passoni

Co-advisor: Prof. Hugo Terças (IST)

Academic year: 2020-2021

1. Introduction

The scientific community is facing problems as the extension of the Standard Model, the unknown Dark Matter, Cosmogenesis and many other. Several theories have been written but only experimental data can confirm their validity, one promising benchmark is studying the neutrino properties [3]. In 2020 it was proposed the neutrino spectra that reaches the Earth [10], it's obtained summing over the three flavor and integrating over the direction, the result shows a flux at energy below the eV. Those neutrino are not detected by the detectors available nowadays since they are not energetic enough to generate a lepton that emits Cherenkov radiation. The scope of this thesis work is to explore a way to detect the neutrino-flux with energy in the range of meV $-$ μeV; we remind that plasmon has energy in the same order of magnitude, therefore we seek for a scheme to make the neutrino flux interacts with the electron plasma. The plasma is a system where the collective behavior prevails, this results in waves that can be excited out of instability as the beam-plasma instability [4]. We work with graphene thanks to the high quality plasmons. The main result is the design of a detector for slow neutrino-flux using a metamaterial-plasma.

2. Plasma and Detection

The Plasma Wave (PW) is generated in the electron (e^-) solid-state plasma, in particular in a graphene sheet where the electron has mass M; the graphene can be used both as single layer or in the Bi-Layer Graphene (BLG) configuration, it's used as channel in a Field-Effect Transistor (FET) configuration as Fig.1. There are source and drain contacts at the edge of the channel of length L, moreover an W thick oxide barrier separates the graphene to the gate contact.
The plasmon can be generated by imposing an modulation (with amplitude V_0) of the source potential [1], or by the Dyakonov-Shur instability [2], or even by coupling an ElectroMagnetic (EM) radiation (if a proper grating structure is used [6], [5]). The generated PW travel along the channel with speed S defined by the system and Boundary Conditions (BC), the plasmon can be detected by the use of Langmuir probe embedded in the FET structure. Other techniques can reveal interesting feature and allow us to better characterize the plasma oscillation. Resonant detection can be performed if the source (drain) is an close (open) circuit. These

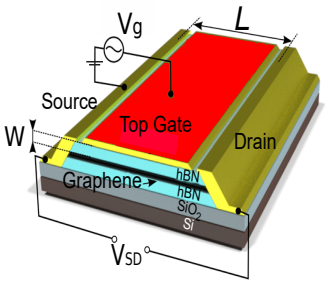

Figure 1: The FET is composed by a channel (length L) at which edges there are Source and Drain contacts, an oxide layer (thickness W) separate the channel to top the Gate. Figures from [1].

asymmetrical BC results in a peaked potential across the channel if the plasmon has frequency equal to the odd harmonics of the channel i.e., $\Omega_j = (2j+1)\pi S/2L$. The responsivity of the system is defined as the V_{SD} normalized by the gate potential V_g [2], it reads as:

$$\mathbb{R} = \left(\frac{S\tau}{L}\right)^2 \frac{(V_0/V_g)^2}{4(\omega-\Omega_j)^2\tau^2+1}, \quad L_{pl} > L, \quad (1)$$

where τ is the momentum relaxation time and the plasmon propagation length $L_{pl} = S\tau$ is the length before attenuation is significant. The detection can be done also by the thermal current (I_{th}) produced by the electrons scattering with the PW, the interference of the wavefront induces a characteristic signal as shown in Fig.2, it require a modification of the FET scheme as explained in [5]. Finally we could use the EM

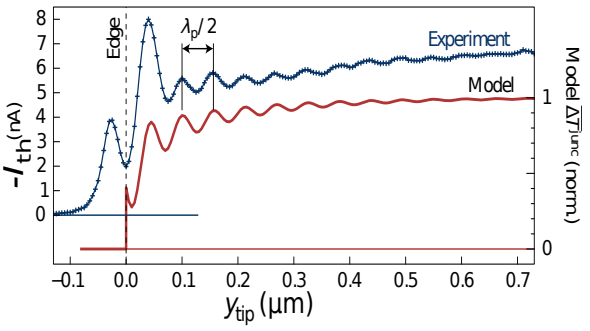

Figure 2: Resulting thermo-current as function of the plasmon origin. The I_{th} shows an oscillation feature caused by the self interference of the plasmon. Figures from [5].

radiation produced by the plasmon decay perform a spectral analysis [9], this is obtained if the radiative decay is favored over the thermal decay. The plasmon detection, regardless the specific technique, requires a Signal to Noise ratio (SN) larger than 1, it will set the constrain on the neutrino flux we can detect.

3. Weak Interaction

The neutrino (ν) is a chargeless lepton with a mass that has to be defined yet, although experimental data constrains its value to be $m < 1$eV. The only way the neutrinos can interact with the electrons is by the weak interaction, it couples the lepton through the Fermi constant G_F. The interaction is described in the Quantum Field Theory by the lagrangian of Eq.(2) [8], it can be reduced to the semiclassical Lagrangian in Eq.(3) by the formal substitutions $\bar{\psi}\gamma_\mu\psi \to \{n; n\,\boldsymbol{v}/c\}$ and $\bar{\psi}\gamma_\mu(1-\gamma_5)\psi \to \{n; n\,\boldsymbol{v}/c\}$, where n ($\boldsymbol{v}$) is the classical density (velocity) of the distribution previously described by the field ψ.

$$L^{\text{int}} = -\tfrac{G_F}{\sqrt{2}}\bar{\psi}_e\gamma^\mu\left[(1-\gamma_5)+(C_V-C_A\gamma_5)\right]\psi_e \times \times \bar{\psi}_\nu\gamma_\mu(1-\gamma_5)\psi_\nu = \quad (2)$$

$$= -\tfrac{G_F}{\sqrt{2}}(C_V+1)\left[n_e n_\nu - \tfrac{(n_e\boldsymbol{v}_e)\cdot(n_\nu\boldsymbol{v}_\nu)}{c^2}\right]. \quad (3)$$

We can derive the Hamiltonian governing the system, it will be useful to derive the force between the two distributions. We can write the electrons (neutrinos) hamiltonian using the free Lagrangian and the L^{int} with the Legendre transformation obtaining the Eqs. (4). We used $\boldsymbol{p}_e = Mn_e\boldsymbol{v}_e$ and $\boldsymbol{p}_\nu = m\gamma_\nu n_\nu \boldsymbol{v}_\nu$ with γ_ν the relativistic correction for the neutrinos.

$$\begin{cases} H_e = \dfrac{p_e^2}{2M} + \tilde{G}_F n_\nu, \\ H_\nu = \sqrt{p_\nu^2c^2 + m^2c^4} + \tilde{G}_F n_e, \end{cases} \quad (4)$$

where we introduced $\tilde{G}_F = G_F(C_V+1)/\sqrt{2}$. The conjugate momentum of specie i, in the presence of species j, reads as $\boldsymbol{P}_i = \boldsymbol{p}_i + \tilde{G}_F\, n_i\, n_j \boldsymbol{v}_j/c^2$. We can thus calculate, by the Hamilton equation $\partial_t \boldsymbol{P}_i = -\boldsymbol{\nabla} H_i$, the time variation of the conjugate momentum; it leads to the force experienced by the particle i due to the Weak interaction with the distribution j [8], the result is Eq.(5),

$$\boldsymbol{F}_i^W = -\tilde{G}_F\left[\boldsymbol{\nabla} n_j + \frac{\partial_t n_j \boldsymbol{v}_j}{c^2}\right]. \quad (5)$$

This force shows that electron and neutrino affect each other and their interaction is symmetric; we must remember that the electron

has a charge therefore it feels also the presence of EM fields, therefore we will consider the $\boldsymbol{F}_e^{EM} = e\boldsymbol{\nabla}\phi$ where ϕ is the sum of the external and self-consistent electric potential. We can now derive the Dispersion Relation (DR) of the system by the use of Kinetic Equations; the system is described by the continuity Eq., the force Eq. and the Maxwell Eqs. For the electrons and neutrinos distributions, the equations are

$$\partial_t n_e + \boldsymbol{\nabla}\cdot(n_e\boldsymbol{v}_e) = 0, \tag{6}$$
$$\partial_t \boldsymbol{v}_e + \boldsymbol{v}_e\cdot\boldsymbol{\nabla}\boldsymbol{v}_e = \frac{\boldsymbol{F}^{\rm EM}+\boldsymbol{F}_e^W}{M}, \tag{7}$$
$$\partial_t n_\nu + \boldsymbol{\nabla}\cdot(n_\nu\boldsymbol{v}_\nu) = 0, \tag{8}$$
$$\partial_t \boldsymbol{v}_\nu + \boldsymbol{v}_\nu\cdot\boldsymbol{\nabla}\boldsymbol{v}_\nu = \frac{\boldsymbol{F}_\nu^W}{m}. \tag{9}$$

The next step is the linearization, we state that the electrons have a non vanishing equilibrium density N_e and a null equilibrium velocity, meanwhile the neutrino have finite equilibrium density N_ν and velocity $\boldsymbol{V}_\nu$. By the formal substitutions $n_e(x,t) \to N_e + n_e(x,t)$, $n_\nu(x,t) \to N_\nu + n_\nu(x,t)$ and $\boldsymbol{v}_\nu(x,t) \to \boldsymbol{V}_\nu + \boldsymbol{v}_\nu(x,t)$ we can rewrite the Eqs.(10)-(13), where we kept only the first order terms. It's worth to notice that the electron-plasma is assumed to be 2D and therefore the Fermi constant must be adjusted to match the dimensional, the result is the formal substitution in $\boldsymbol{F}_\nu^W$ of $\tilde{G}_{\rm F} \to \tilde{g}_{\rm F} \simeq \tilde{G}_{\rm F}/a$ where a is the thickness of the graphene channel.

$$\partial_t n_e + N_e\boldsymbol{\nabla}\cdot\boldsymbol{v}_e = 0, \tag{10}$$
$$\partial_t \boldsymbol{v}_e = \frac{1}{M}\left[e\boldsymbol{\nabla}\phi - \tilde{G}_{\rm F}\left(\boldsymbol{\nabla}n_\nu + \frac{N_\nu\partial_t\boldsymbol{v}_\nu + \boldsymbol{V}_\nu\partial_t n_\nu}{c^2}\right)\right] \tag{11}$$
$$\partial_t n_\nu + N_\nu\boldsymbol{\nabla}\cdot\boldsymbol{v}_\nu + \boldsymbol{V}_\nu\cdot\boldsymbol{\nabla}n_\nu = 0, \tag{12}$$
$$\partial_t \boldsymbol{v}_\nu + \boldsymbol{V}_\nu\cdot\boldsymbol{\nabla}\boldsymbol{v}_\nu = -\frac{\tilde{g}_{\rm F}}{m}\left(\boldsymbol{\nabla}n_e + \frac{N_e\partial_t\boldsymbol{v}_e}{c^2}\right). \tag{13}$$

The four linear differential equations can be reduced to two 2$^{\rm nd}$ diff. equations of two unknown (n_e, n_ν) by eliminating the the velocities $\boldsymbol{v}_e$ and $\boldsymbol{v}_\nu$. Follows the Fourier Analysis of the system stating $\{n_e, n_\nu, \phi\} \propto \exp[i(kx-\omega t)]$, the resulting second order differential system reads as Eqs.(14), (15) where we perform the formal substitutions $\partial_t^2 \to -\omega^2$ and $\nabla^2 \to -k^2$.

$$n_e\omega^2 + \frac{N_e}{M}\left[ek^2\phi + n_\nu\tilde{G}_{\rm F}\left(\frac{\omega^2}{c^2} - k^2\right)\right] = 0 \tag{14}$$
$$n_e\frac{N_\nu\tilde{g}_{\rm F}}{m}\left(\frac{\omega^2}{c^2} - k^2\right) + n_\nu(\omega - V_\nu k)^2 = 0. \tag{15}$$

We still have to evaluated ϕ, it's linked to the electron distribution by the Maxwell equations; we are going to consider two cases, the Gated and Ungated scenario. In the Gated case an electric potential is applied at the gate contact leading to $\phi = -en_e/C$ where C is the capacitance of the Gate-Oxide-Channel structure, moreover the bare DR of gate electron is linear thus implying a non-dispersive plasmon. In case of Ungated structure the Poisson Eq reads as $\phi = -en_e/2\epsilon_0 k$ producing a DR with root square dependency. Notice that the neutrino bare DR is linear with velocity given by V_ν, therefore we expect quite different behavior in case of interaction with gated or ungated electrons. Writing the matrix form of the Eqs.(14), (15) and imposing the determinant to vanish we obtain the Joint Dispersion Relation; it contains the mode that the $\nu - e^-$ system can sustain, they are presented in Fig.3. We see the possibility to generate plasmon out of the instability feature in the Ungated case, the instability comes from the finite imaginary part of the joint DR. This occurs at the intersection of electrons and neutrinos DR; the gated case has real modes and no instability takes place since the bare DRs do not cross.

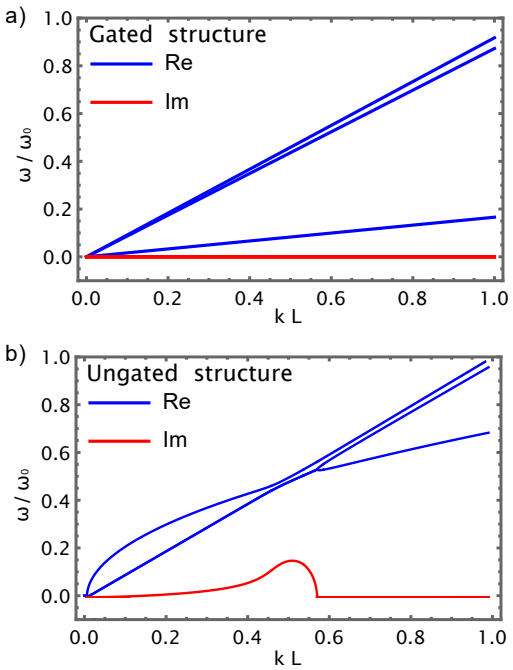

Figure 3: Gated and ungated joint DR with $\omega_0 = c/L \simeq 10$GHz. a) the DR for Gated is Real and Linear, the weak interaction implies only a splitting of the modes; b) the Ungated modes are complex with finite imaginary part around the intersection of the Bare DR of neutrinos and 2D electrons.

4. Metamaterial

For the interaction of the 2D electron with the 3D neutrino flux we needed the Dimensional Reduction to match the different dimension of the two systems. The result is a larger coupling constant $\tilde{g}_{\rm F} \propto a^{-1}$ but the physical cross section of the interaction is almost null since the interaction requires $\boldsymbol{V}_\nu$ in the channel-plane; therefore we define an effective 3D material out of the 2D graphene. We started by considering the Bi-Layer Graphene as basic element -it ensures an constant effective e^- mass- and now we stuck several BLG keeping a buffer layer (thickness d) between each other. The MetaMaterial (MM) dispersion relation is then calculated by considering the mutual EM interaction, increasing the number of layer wee see a convergence of the DR as depicted in Fig.4, We notice that for high wavevector the DR converge to the BLG DR while for low wavevector the DR it has a larger group velocity.

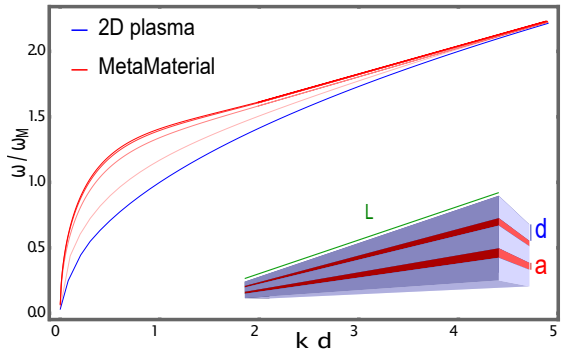

Figure 4: The evolution of the DR from single BLG to metamaterial, the red curve is obtained if the number of layers is larger than 20; in the inset a pictorial representation of the MM with only 2 layers.

To obtain an simpler expression, we focus on the low wavevector limit expanding up to 2nd order the full DR, obtaining Eq.(16). We used adimentional quantities defined by $\tilde{\omega} = \omega/\omega_M$ with $\omega_M^2 = N_e e^2/2M\epsilon_0 d$ and $\tilde{k} = kd$, then the MM optical mode is

$$\tilde{\omega}^2 - \frac{(36-35\tilde{k})^2}{216}\tilde{k} = 0. \qquad (16)$$

We see that the behavior is still as root square with a linear correction, this expression approximates well the DR in the region $k < 0.2d$; we are going to use this expression for study the neutrino-plasma instability.

5. Projection of ν-detector

The interaction is now between the neutrino-flux and the electrons in the MM, we can thus recover the $\tilde{G}_{\rm F}$ in $\boldsymbol{F}_\nu^W$ since both systems are tridimensional, moreover we can define the effective electron density in the MM as $N_e^M = N_e/d$. The DR we are going to solve is Eq.(17) where we introduced the coupling constant $\Gamma = \frac{\tilde{G}_{\rm F}^2 N_\nu N_e^M}{mMc^4}$ and defined the adimensional velocities $(\tilde{V}_\nu, \tilde{c})$ by dividing for $d\,\omega_M$.

$$\left[\tilde{\omega}^2 - \tilde{k}\frac{(36-35\tilde{k})^2}{216}\right](\tilde{\omega} - \tilde{V}_\nu\tilde{k})^2 + \\ -\Gamma(\tilde{\omega}^2 - \tilde{c}^2\tilde{k}^2)^2 = 0 \qquad (17)$$

The interaction, as mention above, bends the bare DR of neutrino and electron making them complex. The solution of Eq.(17) produces the mode showed in Fig.5 where we see the mode α has a positive imaginary part, this is the mode the instability will excite during the neutrino-plasma interaction.

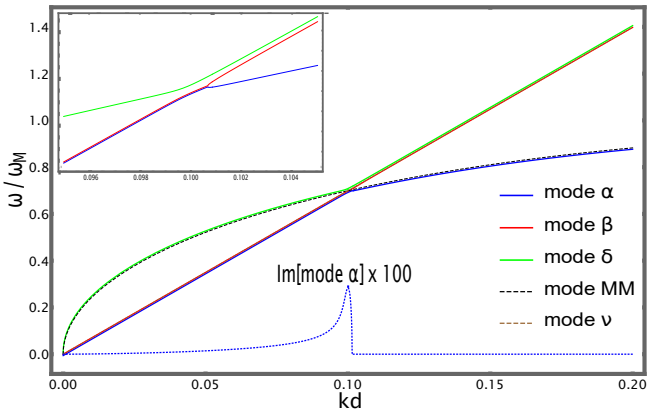

Figure 5: The modes of the neutrino-plasma system, in the inset a zoom in the interception showing the bending of the modes. The imaginary part of mode α is multiplied by 100 for better visibility, it is worth mentioning that the mode β has a negative imaginary part while mode δ is fully real.

The growth rate, $\gamma = \mathrm{Im}(\mathrm{mode}\alpha)$, is responsible of the exponential amplification of the PW, the γ gets bigger when Γ increases i.e., when the neutrino density increases or the mass decreases, assuming $\tilde{V}_\nu$,(Fig.6). We will focus on the plasmon that grows faster, it has wavevector $k_{\rm C}$ and frequency given by $\omega_R + i\gamma_{\rm m}$, we choose to have $k_{\rm C} = 0.1/d$.

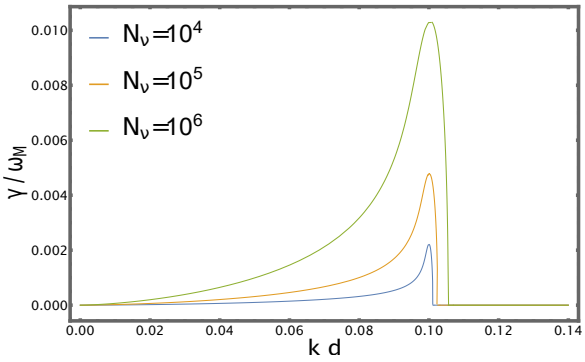

Figure 6: The γ amplitude and width depends on the parameter Γ, here the result for $N_e = 10^{15}\mathrm{m}^{-2}$, $M \simeq 0.018\mathrm{MeV}$, $d \simeq 0.4\mu\mathrm{m}$, $m = 0.01\mathrm{eV}$ and $V_\nu = 0.1\,c$ and some N_ν.

The complex frequency implies that the plasmon density not only oscillates but also grows exponentially as

$$n_e(x,t) = n_e^0 \exp[i(k_C x - \omega_R t)] \exp(\gamma_\mathrm{m} t), \quad (18)$$

where n_e^0 is the amplitude given by the thermal noise. To actually compute the SN of the plasmon we must specify the plasma and neutrino parameters, we consider a plasma with $N_e = 10^{15}\,\mathrm{m}^{-2}$ and $M \simeq 0.018\,\mathrm{MeV}$, the MM has $d \simeq 0.4\,\mu\mathrm{m}$, while the neutrino is characterized by $m = 0.01\,\mathrm{eV}$ and $V_\nu = 0.1c$. We want to generate a plasmon with amplitude hundred time larger than the initial one, this requires $\exp(\gamma_\mathrm{m} t_D) = 100$ where t_D is the time that the neutrino-flux spends inside the MM interacting with the electrons i.e., $t_D \simeq L/V_\nu$. These request sets the length of the MM: it depends on the neutrino density because N_ν and $\tilde{V}_\nu$, define the γ_m. It is worth to remind the detectability is related to the Signal to Noise ratio defined as

$$\mathrm{SN} = 10 \log_{10}\left[\exp\left(2\frac{\gamma_\mathrm{m} \mathrm{L}}{\mathrm{V}_\nu}\right)\right]. \quad (19)$$

In case of neutrinos at $10^{-4}\mathrm{eV}$ and $N_\nu = 10^4\mathrm{m}^{-3}$ the MM is approximately 1cm long with $SN > 1$, for $N_\nu = 10^{-2}\mathrm{m}^{-3}$ we need a MM of 1m to get the same amplification. The neutrino can have different energy and the γ_m dependents on that. We start assuming $L = 1\mathrm{cm}$ while the neutrino has $m = 0.01\mathrm{eV}$ and $N_\nu = 10^4\mathrm{m}^{-3}$; the kinetic energy of the flux varies from $10^{-7}\,\mathrm{eV}$ to $1\,\mathrm{eV}$; the resulting parameters are shown in Fig.7. Increasing the energy the V_ν increases and thus the t_D decreases and so we expect a reduction of the γ_m; trying to compensate, we increases the N_e as the ν energy increases -to increase Γ but the γ_m still decreases. The consequence is a reduction of the SN as the ν energy increases, therefore the more energetic neutrinos are unlikely to be detected with this technique.

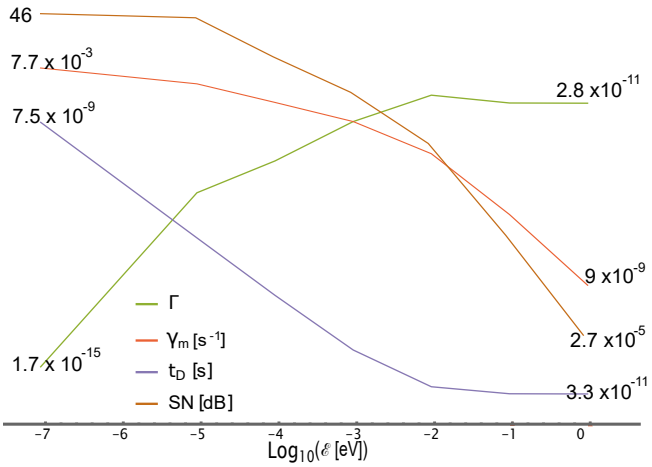

Figure 7: Evolution of the instability parameters as function of the neutrino kinetic energy for $L = 1\mathrm{cm}$, $N_\nu = 10^4\mathrm{m}^{-3}$ and $m = 0.01\mathrm{eV}$.

Finally we evaluate the SN varying both energy and flux of the neutrino, the SN is presented in Fig.8 using the quantity $\Phi = N_\nu V_\nu$. It is straightforward to see that larger flux are more easy to be detected, on the contrary, increasing the energy reduces drastically the SN making virtually impossible to detect neutrino with energy above the eV: this instability detection technique is suitable for ultra-low energetic ν-flux.

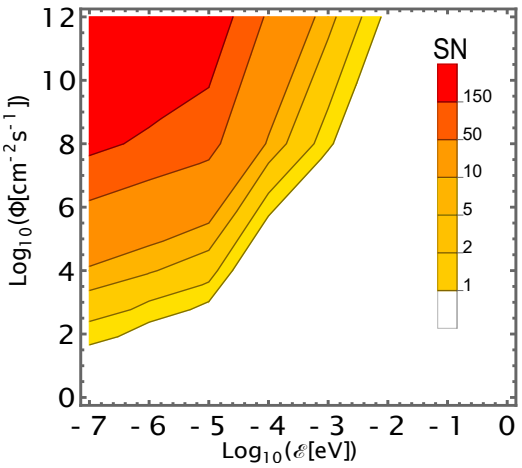

Figure 8: Evolution of the SN for $L = 1\mathrm{cm}$, $m = 0.01\mathrm{eV}$ and for N_e that increase from $10^{11}\mathrm{m}^{-2}$ to $10^{16}\mathrm{m}^{-2}$ to try compensate the decreasing t_D.

6. Conclusions and Future

The weak interaction generate a ponderomotive-like force between solid-state plasma and neutrino flux, with the kinetic theory we derived the joint dispersion relation that has an imaginary component. The resulting instability is able to generate plasmons, in particular we considered the electrons in the metamaterial obtained by a graphene metamaterial; the graphene has metallic contact at the edge to create a FET-like structure, this can be used to detect the plasmons and thus infer on the neutrino flux properties. Several assumptions have been made during this thesis work and we will analysis in future works their consequences; in particular in all calculation the neutrino mass was assumed to be constant, it must be taken into account its unknown value along with the flavor oscillation in the presence of medium and EM fields. There's the possibility for the plasmon to force an flavor-oscillation in the neutrino-flux. The DR was obtained in the linear perturbation approach leading to a constant growth rate, non linear terms must be taken into account to find the saturation of the instability; we can consider the MM at ultra-low temperatures to avoid the saturation. The assumption of initial plasma at rest could be relaxed to see if the instability benefit from that, look for appendix A for the additional term in the $\boldsymbol{F}^W$ we neglect. Moreover it was not considered the decay of the plasmon, future works must examine its consequences on the signal to noise ratio. So far it seems that our scheme is the first proposal to detect neutrino with energy below the eV by plasma-interaction, we therefore see large room for improvement. The study of low energetic neutrino can set constrains on the theories beyond the Standard Model, it will helpful to set boundary for the neutrino mass; lastly but not least the measurement of slow neutrino can implies the existence of the so-called Relic Neutrino, therefore helping in the Dark Matter solution and Early-Universe models.

7. Acknowledgements

I thank Instituto Superior Tecnico and Politecnico di Milano, alongside the Double Degree Program, for all the support in the last three years.

References

[1] D.A. Bandurin, D. Svintsov, I. Gayduchenko, and et al. Resonant terahertz detection using graphene plasmons. *Nature Communications*, 2018. doi: 10.1038/s41467-018-07848-w.

[2] M.I. Dyakonov and M.S. Shur. Plasma wave electronics: Novel terahertz devices using two dimentional electron fluid. *IEEE Trans. Electron Dev.*, 1996. doi: 10.1109/16.536809.

[3] C. Giunti and C.W. Kim. *Fundamental of Neutrino Physics and Astrophysics*. Oxford University Press, 2007.

[4] M.R. Gupta. Nonlinear stabilization of cold bema-plasma instability. *J. Plasma Physics*, 1972. doi: 10.1017/S0022377800007042.

[5] M.B. Lundeberg, Y. Gao, A. Woessner, and et al. Thermoelectric detection and imaging of prpagating graphene plasmons. *Nature materials*, 2017. doi: 10.1038/NMAT4755.

[6] K.V. Mashinsky, D.V. Fateev, and V.V. Popov. Graphene plasmonic terahertz detector with high responsivity. *J. Phys.: Conf. Ser.*, 2017. doi: 10.1088/1742-6596/917/6/062045.

[7] A.H. Castro Neto and et al. The electronic properties of graphene. *Reviews of Modern Physics*, 2009. doi: 10.1103/RevModPhys.81.109.

[8] L.O. Silva, R. Bingham, J.M. Dawson, and et al. Collective neutrino-plasma interaction. *Physics of Plasma*, 1999. doi:10.1063/1.874037.

[9] H. Terças, J.D. Rodrigues, and J.T. Mendonça. Axion-plasmon polaritons in strongly magnetized plasmas. *Physical Review Letters*, 2018. doi: 10.1103/PhysRevLett.120.181803.

[10] E. Vitagliano, I. Tamborra, and G. Raffelt. Grand unified neutrino spectrum at earth: Sources and spectral components. *Reviews of Modern Physics*, 2020. doi:10.1103/RevModPhys.92.045006.